

Quantum State Preparation via Schmidt Spectrum Optimisation

Josh Green,^{1,*} Josh Snow,^{1,†} and Jingbo Wang^{1,‡}

¹*Centre for Quantum Information, Simulation and Algorithms,
School of Physics, Mathematics and Computing,
The University of Western Australia, Perth, Australia*

Abstract

We introduce an efficient algorithm for the systematic design of shallow-depth quantum circuits capable of preparing many-body quantum states represented as Matrix Product States (MPS). The proposed method leverages Schmidt spectrum optimization (SSO) to minimize circuit depth while preserving the entanglement structure inherent to MPS representations, thereby enabling scalable state preparation on near-term quantum hardware. The core idea is to *disentangle* the target MPS using a sequence of optimised local unitaries, and then reverse this process to obtain a state preparation circuit. Specifically, we define a loss function directly on the Schmidt spectra of intermediate states and use automatic differentiation to optimise each circuit layer so as to systematically reduce entanglement entropy. Once a disentangling sequence has been learned, we take the adjoints of the optimised unitaries to obtain a shallow-depth circuit that approximately reconstructs the target MPS from the computational all-zero state. We benchmark SSO across a range of MPS approximations to the ground states of local Hamiltonians and demonstrate state-of-the-art shallow-depth performance, improving accuracy by up to an order of magnitude over existing methods. Finally, we provide numerical evidence that SSO mitigates the adverse time-complexity scaling observed in previous disentangling-based approaches.

1. Introduction

Quantum state preparation refers to the process of transforming a quantum system from its initial all-zero state into a precisely defined configuration—such as approximations of highly structured many-body systems, image or signal data encoding, or discretized special functions—that serves as the required input for a quantum computation. This task is fundamental to quantum algorithm design, as the efficiency and accuracy of state preparation directly influence the overall performance and scalability of quantum computations. Tensor networks (TNs) provide an efficient framework for representing complex quantum states in a compact classical form, making them a natural foundation for designing shallow-depth quantum circuits capable of preparing complex and entangled states. This connection has motivated extensive research into the preparation of various TN architectures, with particular emphasis on Matrix Product States (MPS) [1–7], as well as Tree Tensor Networks (TTN) [8], the Multi-Scale Entanglement Renormalization Ansatz (MERA) [9], and, more recently, two-dimensional isometric Projected Entangled Pair States (isoPEPS) [10].

The MPS is one of the most widely studied of all TNs, providing an efficient representation of certain classes of one-dimensional area-law quantum states, such as the ground states of gapped local Hamiltonians

* josh.green@uwa.edu.au

† josh.snow@uwa.edu.au

‡ jingbo.wang@uwa.edu.au

[11, 12]. The MPS possesses many advantageous computational features, such as the ability to efficiently compute canonical forms and Schmidt decompositions across its bipartitions. Despite being formally tailored to one-dimensional systems, these powerful computational features often make MPS the leading ansatz in the numerical study of certain two-dimensional quantum systems, such as the 2D Hubbard or Heisenberg models [13–15].

It is well-known that any one-dimensional isometric TN with bond dimension χ can be realised by a quantum circuit through the embedding of all tensors into $\mathcal{O}(\log_2 \chi + 1)$ -qubit gates [1]. The topology and circuit depth of such a mapping typically matches the topology of the TN itself (i.e., linear-depth for MPS, logarithmic for TTN and MERA with each branch being prepared in parallel). However, the decomposition of multi-qubit gates into smaller, physically realisable gates can lead to significant computational overhead [16–18]. For example, although exact MPS synthesis scales efficiently as $\mathcal{O}(n\chi^2)$, the requirement for decomposing multi-qubit gates typically leads to significantly deeper-than-necessary quantum circuits [19].

The first significant work-around to multi-qubit decompositions was the development of the Matrix Product Disentangler (MPD) algorithm, designed to approximately disentangle an MPS towards a product state using sequential layers of local one- and two-qubit gates [18]. After the MPD is computed, the disentangling process can be reversed, generating a circuit that progressively reconstructs the entanglement of the target MPS. However, the MPD algorithm is pathological: Its success depends on the assumption that the operator that disentangles a low-rank MPS approximation can also effectively disentangle the MPS it approximates, which is not generally true. Further, the MPD often suffers from an exponential scaling of computational resources with the number of circuit layers, largely owing to the suboptimality of the disentangling process [3, 19].

We introduce Schmidt Spectrum Optimisation (SSO) as an improved framework for quickly disentangling MPS using sequential circuit layers. In SSO, disentangling is reformulated as an optimisation problem defined explicitly on the Schmidt spectra of intermediate MPS in the disentangling process. Using efficient tensor contractions, we employ automatic differentiation to compute stable gradients that relate changes in the Schmidt spectra to the parameters of each circuit layer. This enables iterative optimisation of layers that progressively shape the Schmidt spectra toward a desired distribution. For state preparation, we choose a loss that maximises the weight of the first two Schmidt coefficients across all bipartitions. Much like in the MPD algorithm, the disentangling process can be reversed to generate an efficient state preparation circuit.

We empirically demonstrate that SSO reduces the entanglement of an MPS much more rapidly than the MPD algorithm, yielding significantly stronger disentangling at fixed circuit depth. As a consequence, SSO mitigates pathological behaviour associated with the worst-case exponential growth of bond dimension with the number of circuit layers – an artefact of repeatedly contracting the MPS with ineffective disentangling layers. In addition, we show that SSO substantially outperforms optimised variants of MPD, in which the MPD algorithm is used to initialise a subsequent optimisation that maximises the overlap between a parametrised tensor-network representation of the circuit and the target MPS. Moreover, when such fidelity-maximising optimisation is applied as a post-processing step, SSO provides a far better initialisation of circuit parameters, leading to faster convergence and higher-fidelity local minima.

We evaluate SSO on a range of state preparation tasks, including ground-state MPS approximations to three one-dimensional local Hamiltonians (Ising, many-body-localised, and Hubbard models). We

further test its performance on an MPS approximation to the ground state of a modest two-dimensional Heisenberg model. Across these benchmarks, we find that the SSO algorithm achieves state-of-the-art shallow-depth performance, improving accuracy by up to an order of magnitude and markedly alleviating critical numerical scaling issues.

2. Relation to Previous Work

We now contextualise our work in relation to previous MPS-based state preparation approaches to clarify the scope, novelty, and core advantages of the Schmidt Spectrum Optimisation algorithm.

2.1 Exact Synthesis and Parallelisation of MPS

It is well known that any MPS of bond dimension χ can be prepared exactly by a single sequential (staircase) circuit of local $\mathcal{O}(\log_2 \chi + 1)$ -multi-qubit gates [1]. More recently, Malz *et al.* [5] have shown that this linear-depth scaling is not fundamental: for translation-invariant normal MPS, they prove a lower bound $T = \Omega(\log N)$ on the circuit depth of any local-unitary preparation protocol and construct a renormalisation-group-inspired algorithm that prepares such states with error ϵ in depth $T = \mathcal{O}[\log(N/\epsilon)]$, which is optimal. Their scheme can be further accelerated using mid-circuit measurements and feedback, achieving depth $T = \mathcal{O}[\log \log(N/\epsilon)]$ in this adaptive setting and extending to a broader class of (including some non-normal and inhomogeneous) MPS.

Complementary to these log-depth constructions, Smith *et al.* [6] show that adaptive circuits combining local unitaries, mid-circuit measurements and feedforward can exactly prepare a broad class of MPS in *constant* depth, including short- and long-range entangled phases, symmetry-protected/topological states and MBQC resource states. Exploiting global on-site symmetries, they characterise when constant-depth preparation is possible and give explicit adaptive protocols that outperform any unitary-only scheme. Taken together, these works establish tight asymptotic depth bounds for exact preparation of structured MPS families. By contrast, here we address the *approximate*, shallow-depth preparation of generic target MPS using fixed two-qubit gate layers, where constant or logarithmic depth is typically unattainable and the central challenge is to obtain numerically stable, high-fidelity circuits under strict depth constraints.

2.2 The MPD Algorithm and its Pathologies

Decomposing the multi-qubit gates in the exact MPS synthesis circuit into one- and two-qubit gates yields a circuit of depth $\mathcal{O}(n\chi^2)$. While efficient in complexity terms, this decomposition introduces a large constant overhead in practice [17]. This motivated the MPD algorithm, which bypasses transpilation by directly constructing a state-preparation circuit of one- and two-qubit gates at the expense of an approximation error [18]. In many cases, MPD yields shallower depth circuits than the exact decomposition [19].

In MPD, the intermediate MPS $|\psi^{(k)}\rangle$ at disentangling layer k is compressed to its optimal $\chi = 2$ approximation $|\tilde{\psi}^{(k)}\rangle$. The k^{th} disentangling operator is then defined such that

$$U_k |\tilde{\psi}^{(k)}\rangle = |0\rangle^{\otimes n} \quad (1)$$

where U_k is implemented as a single layer of local $SU(4)$ gates. Since $|\tilde{\psi}^{(k)}\rangle$ *approximately* mirrors the entanglement structure of $|\psi^{(k)}\rangle$, U_k is expected to roughly disentangle $|\psi^{(k)}\rangle$. The intermediate state is

then updated as

$$|\psi^{(k+1)}\rangle \leftarrow U_k |\psi^{(k)}\rangle \quad (2)$$

and the disentangling process is repeated for $k = 1, \dots, L$. The adjoint circuit acts such that

$$U_1^\dagger U_2^\dagger \cdots U_L^\dagger |0\rangle^{\otimes n} \approx |\psi^{(1)}\rangle \quad (3)$$

where $|\psi^{(1)}\rangle$ is the target MPS. We define the accuracy of this state preparation protocol using the fidelity $F := |\langle \psi^{(1)} | U_1^\dagger U_2^\dagger \cdots U_L^\dagger |0\rangle|^2$.

The MPD approach suffers from two key pathologies. First, U_k effectively disentangles $|\psi^{(k)}\rangle$ when the fidelity

$$F_{\chi=2} = |\langle \psi^{(k)} | \tilde{\psi}^{(k)} \rangle|^2 \quad (4)$$

is close to 1. As $F_{\chi=2} \rightarrow 0$, the entanglement structure of $|\tilde{\psi}^{(k)}\rangle$ ceases to be representative of $|\psi^{(k)}\rangle$, and U_k becomes an ineffective disentangler. For many physically relevant target MPS of interest, $F_{\chi=2}$ is small, so the MPD is ineffective at disentangling them.

Second, if $|\psi^{(k)}\rangle$ has bond dimension $\chi^{(k)}$, then applying U_k yields a state $|\psi^{(k+1)}\rangle$ with bond dimension $\chi^{(k+1)} = 2\chi^{(k)}$. When disentangling succeeds, $\chi^{(k+1)}$ can often be truncated back down without loss. However, in the worst case, this leads to exponential growth of the bond dimension with the number of layers L . A more detailed analysis of these pathologies is provided in [19].

2.3 Tensor Network Optimisation (TNO) Approaches

More recent work has proposed preparing MPS using fully classical tensor network optimisation (TNO) frameworks, in which the parametrised quantum circuit is represented explicitly as a tensor network [2, 3, 7]. Since the target state is an MPS, the fidelity

$$F_S = |\langle \psi_{\text{targ}} | U(\theta) | 0^{\otimes n} \rangle|^2 \quad (5)$$

can be evaluated entirely classically. However, many TNO approaches are known to suffer from optimisation pathologies, including severe local minima [19] and loss landscapes that exhibit features analogous to barren plateaus [20]. Fortunately, the MPD algorithm can be used to initialise TNO parameters $\theta_0 = \theta_{\text{MPD}}$, which has been shown to significantly improve optimisation outcomes [2, 3, 19]. We consider these optimised variants of the MPD algorithm when benchmarking the SSO in Section 5.

2.4 Novelty and Advantages of Schmidt Spectrum Optimisation

SSO has several intuitive advantages over standard MPD and MPD+TNO methods. These benefits arise from the fundamentally different way SSO approaches the disentangling problem, enabling stronger and more reliable performance. The advantages can be grouped into three key improvements:

1. Disentangling by direct optimisation. SSO avoids the heuristic assumption that a disentangler optimised for a low-rank approximation (e.g. $\chi = 2$) will also effectively disentangle the full MPS. Instead, we directly optimise for disentangling by extremising a loss function defined explicitly on the Schmidt spectra. The SSO, therefore, does not require the target state to have high $F_{\chi=2}$. We also empirically

demonstrate that SSO significantly mitigates issues related to the bond dimension growing for intermediate disentangling states, owing to the computation of more effective disentangling layers.

2. Escaping fidelity-driven path dependence. In fidelity-maximising TNO approaches, each optimisation step is constrained to keep the output state close to the target, since the objective is to maximise the fidelity. In contrast, SSO replaces this fidelity objective with a loss defined on the Schmidt spectra, and explicitly allows intermediate states to move away from the target as long as they substantially reduce entanglement.

3. Layerwise optimisation and improved initialisation for TNO. Each circuit layer in SSO is optimised independently while all other layers are held fixed. By achieving strong disentangling in this layerwise manner, we greatly reduce the need for global optimisation over all layers with a fidelity-based objective, which becomes increasingly challenging as depth grows. However, if the total number of layers is small, then the fidelity-maximising TNO can be used as a post-processing step. We denote this post-processed variant of SSO as SSO+All. SSO provides an improved initialisation of parameters for TNO, significantly improving training outcomes.

3. Preliminaries

We provide a minimal background on the form, Schmidt decomposition, and bond dimension truncation of matrix product states. For a more rigorous theoretical background, we point the reader to [21, 22].

3.1 Matrix Product States (MPS)

Definition. Consider a one-dimensional quantum system of n sites with local Hilbert space \mathbb{C}^d and computational basis $\{|i\rangle\}_{i=0}^{d-1}$. For qubits, $d = 2$. A Matrix Product State (MPS) with open boundary conditions and virtual dimensions $\{\alpha_j\}_{j=0}^n$ (with $\alpha_0 = \alpha_n = 1$) is the variational ansatz

$$|\psi\rangle = \sum_{i_1, \dots, i_n=0}^{d-1} \sum_{\{\alpha_j\}} A_{\alpha_0, \alpha_1}^{[1] i_1} A_{\alpha_1, \alpha_2}^{[2] i_2} \cdots A_{\alpha_{L-1}, \alpha_L}^{[n] i_n} |i_1 i_2 \cdots i_L\rangle, \quad (\alpha_0 = \alpha_n = 1). \quad (6)$$

where for each site j and physical index i_j , $A_{\alpha_{j-1}, \alpha_j}^{[j] i_j} \in \mathbb{C}^{\alpha_{j-1} \times \alpha_j}$ is a complex matrix [21]. The bond dimension $\chi := \arg \max_j \alpha_j$ is defined as the maximum virtual dimension in the MPS. The MPS contains $\mathcal{O}(2n\chi^2)$ parameters, and χ controls the expressivity of the MPS.

Canonical form. An MPS is said to be in left-canonical form up to site m if, for each $j \leq m$,

$$\sum_{i=0}^{d-1} (A^{[j] i})^\dagger A^{[j] i} = I_{\alpha_j}. \quad (7)$$

The left-canonical constraint in (7) states that the linear map from the left bond space to the composite (right bond \otimes physical) space is an isometry. Similarly, right-canonical tensors satisfy $\sum_i A^{[j] i} (A^{[j] i})^\dagger = I_{\alpha_{j+1}}$. Any MPS with open-boundary conditions can be put into canonical form using successive QR or SVD factorisations with $\mathcal{O}(n\chi^3)$ complexity [23].

3.2 Schmidt Decomposition and Truncation Error

Schmidt decomposition. Given a bipartition of the n -qubit system into subsystems A and B (for instance, $A = \{1, \dots, m\}$ and $B = \{m+1, \dots, n\}$), any pure state $|\psi\rangle \in \mathcal{H}_A \otimes \mathcal{H}_B$ admits a Schmidt decomposition

$$|\psi\rangle = \sum_{k=1}^r \lambda_k |\Phi_k\rangle_A \otimes |\Phi_k\rangle_B, \quad (8)$$

where the Schmidt coefficients $\lambda_k \geq 0$ are non-increasing, satisfy $\sum_k \lambda_k^2 = 1$, and $r = \text{rank}(\rho_A) = \text{rank}(\rho_B)$ is the Schmidt rank. We denote the square of Schmidt coefficients, $p_k := \lambda_k^2$, as the Schmidt probabilities. The von Neumann entanglement entropy across the bipartition is

$$S(A:B) = - \sum_k p_k \log p_k \leq \log r \leq \log \alpha_m, \quad (9)$$

where α_m is the bond dimension of the virtual index cut by the bipartition. The Schmidt spectrum $\{\lambda_k\}_k$ completely characterises the entanglement across that cut [22]. An example Schmidt decomposition across the central bipartition of a 6-site MPS is visualised in Fig. 1.

Computing the Schmidt decomposition. For an MPS, the bipartition $A|B$ induced by cutting a single virtual bond can be put in *mixed canonical form*. In practice, one left-orthonormalises tensors on A and right-orthonormalises tensors on B via successive QR or SVD steps. The tensor at the cut is then reshaped into a matrix and decomposed with a single SVD; its singular values are exactly the Schmidt coefficients for that bipartition. Further details can be found in [21–23].

Bond-dimension truncation. Consider truncating the virtual bond associated with $A|B$ from bond dimension α_m to $\alpha'_m < \alpha_m$. The Frobenius-norm optimal approximation is obtained by retaining only the α'_m largest Schmidt coefficients [24, 25]. If we order the coefficients such that $\lambda_1 \geq \lambda_2 \geq \dots \geq \lambda_{\alpha_m}$, the truncation error is

$$\varepsilon_{\text{disc}}(\alpha'_m) := \sum_{k>\alpha'_m} p_k = \sum_{k>\alpha'_m} \lambda_k^2, \quad (10)$$

which equals the squared norm of the discarded component. The fidelity between the state $|\psi\rangle$ and the (renormalised) truncated state $|\psi_{\chi'}\rangle$ is then $F(\alpha'_m) = 1 - \varepsilon_{\text{disc}}(\alpha'_m)$.

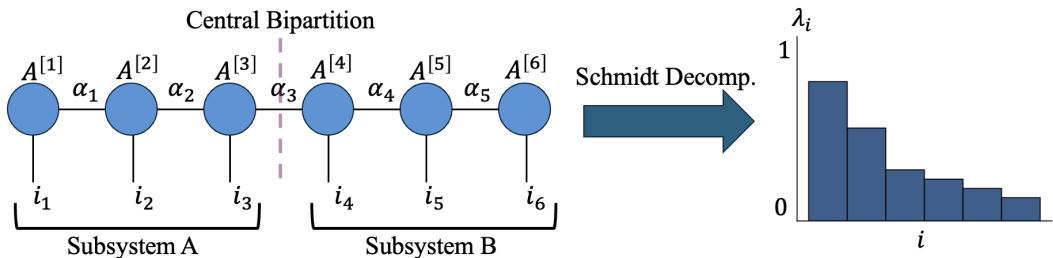


FIG. 1: Computing the Schmidt decomposition for a specified bipartition of the MPS with virtual dimension $|\alpha_j|$ generates a vector of $|\alpha_j|$ non-increasing, non-negative Schmidt coefficients, which are used to define the loss function in the SSO algorithm. Here we visualise the Schmidt spectrum corresponding to the central bipartition (across α_3) for a random real-valued MPS with $n = 6$, $\chi = 6$.

4. Description of the SSO Algorithm

We now present a detailed description of the Schmidt Spectrum Optimisation (SSO) algorithm. We describe the structure of SSO, examine its cost function, explore post-processing strategies, and discuss its computational complexity, situating the method within the broader landscape of tensor-network optimisation.

4.1 Schmidt Spectrum Optimisation (SSO)

Let $|\psi^{(k)}\rangle$ be an n -qubit quantum state represented as an MPS with bond dimension $\chi^{(k)}$. For each bipartition between sites i and $i+1$ there is a Schmidt decomposition with Schmidt values $\{\lambda_{i,j}^{(k)}\}$, which we collect into a vector $\vec{\lambda}_i^{(k)}$ ordered such that $\lambda_{i,1}^{(k)} \geq \lambda_{i,2}^{(k)} \geq \dots \geq \lambda_{i,|\alpha_i|}^{(k)}$ and $\sum_{j=1}^{|\alpha_i|} \left(\lambda_{i,j}^{(k)}\right)^2 = 1$. We denote the full set of Schmidt spectra across all $n-1$ possible bipartitions of $|\psi^{(k)}\rangle$ by $\boldsymbol{\lambda}^{(k)} = \{\vec{\lambda}_i^{(k)}\}_{i=1}^{n-1}$.

Starting with a target MPS $|\psi^{(1)}\rangle$, the objective of SSO is to optimise L layers of local unitaries $\{U_k(\theta_k)\}_{k=1}^L$ that sequentially remove entanglement from the state. Specifically, the objective at iteration k is to optimise θ_k such that the updated state

$$|\psi^{(k+1)}\rangle = U_k(\theta_k) |\psi^{(k)}\rangle \quad (11)$$

has Schmidt spectra $\boldsymbol{\lambda}^{(k+1)}$ that extremise a cost function $C(\boldsymbol{\lambda}^{(k+1)})$.

We adopt the (staircase) circuit ansatz $U_k(\theta_k)$ consisting of a single layer of parameterized $SU(4)$ gates, which is the $\chi = 2$ circuit subclass of Matrix Product Unitary (MPU) [26]:

$$U_k(\theta_k) = \prod_{i=1}^{n-1} \left(\mathbb{I}^{\otimes(i-1)} \otimes U^{[i,i+1]}(\theta_{k,i}) \otimes \mathbb{I}^{\otimes(n-i-1)} \right) \quad (12)$$

where each 2-qubit gate $U^{[i,i+1]}(\theta_{k,i})$ requires 15 parameters to fully parameterize.

To evaluate the cost $C(\boldsymbol{\lambda}^{(k+1)})$ and its gradients, we need access to the Schmidt spectra of $|\psi^{(k+1)}\rangle$. The staircase ansatz in Eq. 12 allows each two-qubit gate $U^{[j,j+1]}(\theta_{k,j})$ to be locally contracted with the neighbouring MPS tensors with physical indices i_j and i_{j+1} . This keeps $|\psi^{(k+1)}\rangle$ in MPS form using only local contractions, so $|\psi^{(k+1)}\rangle$ can be brought into mixed canonical form and the Schmidt values $\{\lambda_{i,j}^{(k+1)}\}$ can be computed. Automatic differentiation through these tensor contractions yields stable gradients $\nabla_{\theta_k} C(\boldsymbol{\lambda}^{(k+1)})$, and the circuit parameters θ_k can be trained via gradient descent [27]. This methodology is summarised in Fig. 2.

4.2 Loss Function and Optimisation

We choose a loss function that encourages each bipartition of $|\psi^{(k+1)}\rangle$ to be well approximated by a rank-2 truncation. The optimal $\chi = 2$ truncation error at bond i is given by

$$\epsilon_i^{(k+1)} = \sum_{j>2} \left(\lambda_{i,j}^{(k+1)}\right)^2 = 1 - \left(\lambda_{i,1}^{(k+1)}\right)^2 - \left(\lambda_{i,2}^{(k+1)}\right)^2 \quad (13)$$

where $\lambda_{i,1}^{(k+1)}$ and $\lambda_{i,2}^{(k+1)}$ are the largest and second largest coefficients of the Schmidt decomposition between sites i and $i+1$, respectively. We define the layer- k loss as the sum of these local truncation

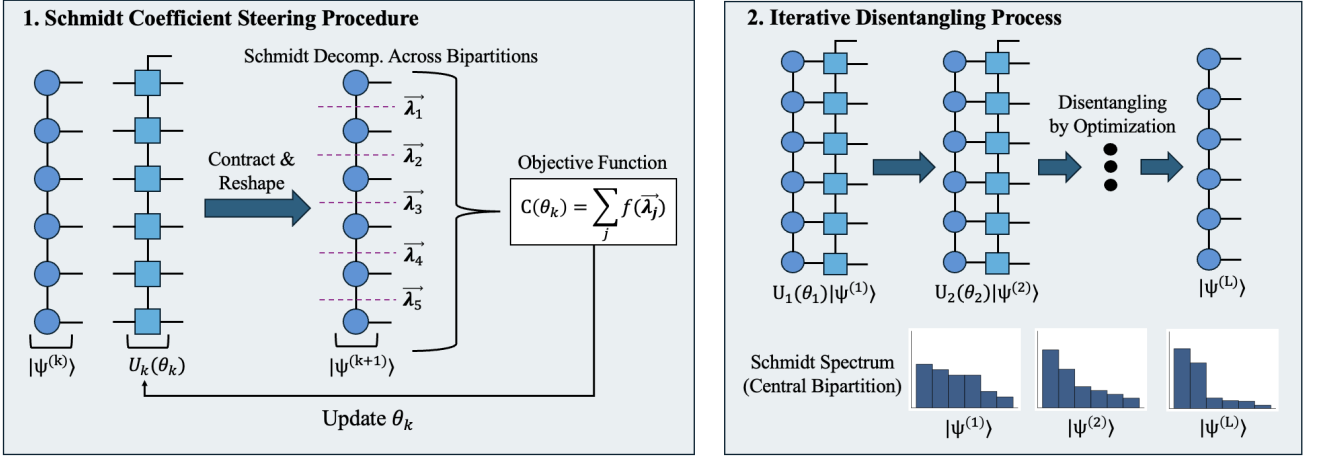


FIG. 2: The *Schmidt Spectrum Optimisation* (SSO) algorithm. The parameterized circuit layer $U_k(\theta_k)$ is contracted with the intermediate MPS $|\psi^{(k)}\rangle$ producing an updated MPS $|\psi^{(k+1)}\rangle$. The Schmidt decomposition is computed across all bipartitions of $|\psi^{(k+1)}\rangle$, and the circuit parameters θ_k are updated via gradient descent to minimise the specified objective function. The specific objective function we introduce in Eq. 14 corresponds to $f(\vec{\lambda}_j) = \vec{\lambda}_{1,j}^2 + \vec{\lambda}_{2,j}^2$. By repeating this process, the MPS is iteratively disentangled.

errors over all bonds:

$$C(\boldsymbol{\lambda}^{(k+1)}) = \sum_{i=1}^{n-1} 1 - \left(\lambda_{i,1}^{(k+1)}\right)^2 - \left(\lambda_{i,2}^{(k+1)}\right)^2 \quad (14)$$

This loss is implicitly parameterized by θ_k . Minimising the loss in Eq. 14 amounts to maximising, at each bond, the weight retained by the leading two Schmidt coefficients, and hence minimising the local truncation error of the $\chi = 2$ approximation to $|\psi^{(k+1)}\rangle$. See a visualisation of the concentration of the Schmidt weight in the leading two coefficients for a 6-site random MPS in Fig. 3.

We initialise each circuit layer by sampling $\theta_k \sim \mathcal{N}(0, 10^{-3})$ such that $U_k(\theta_k) \approx \mathbb{I}_{2^n}$ and $\boldsymbol{\lambda}^{(k+1)} \approx \boldsymbol{\lambda}^{(k)}$ at initialisation. This prevents the initial entanglement growth that would be induced by a random parameter initialisation. We learn parameters using L-BFGS-B. While Eq. 14 is designed for the fast disentangling of the MPS via a $\chi = 2$ approximation, the described SSO framework is compatible with any loss that can be efficiently computed from the Schmidt spectra. For example, one could directly minimise the mean entanglement entropies across all bipartition, or adopt other model-specific objectives. In this work, we adopt the specific form in Eq. 14 because, as we demonstrate, it leads to highly effective preparation circuits with shallow-depth constraints.

4.3 Quantum State Preparation

The overall objective of SSO is to compute a set of L efficient unitary operators $\{U_k\}_{k=1}^L$ that sequentially disentangle the target MPS $|\psi^{(1)}\rangle$. After L iterations we obtain

$$|\psi^{(L)}\rangle = U_L \cdots U_2 U_1 |\psi^{(1)}\rangle \quad (15)$$

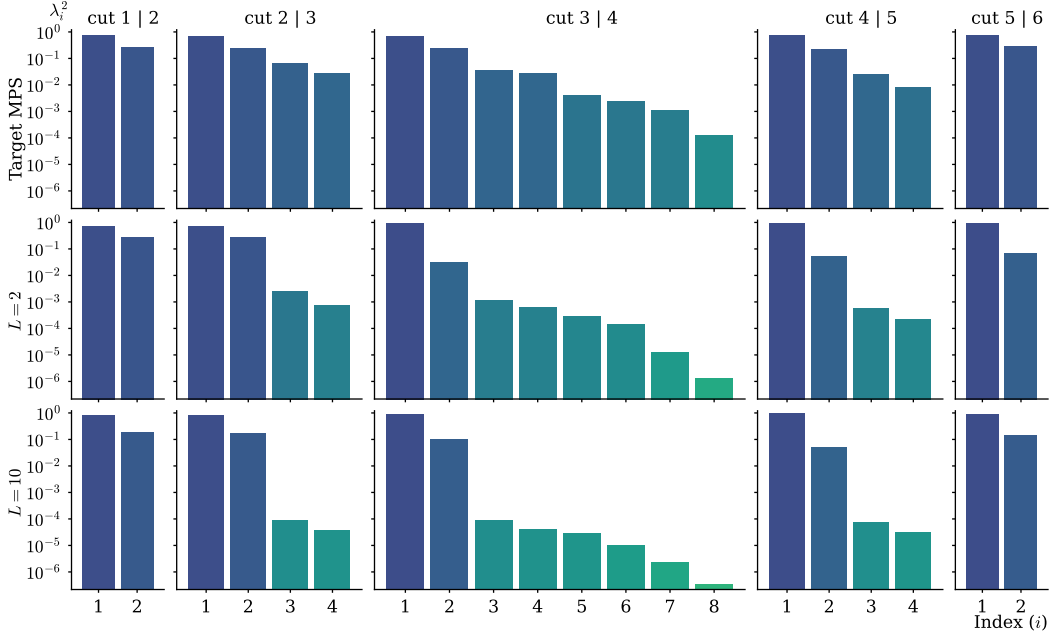


FIG. 3: The normalised Schmidt probabilities (λ_i^2) across each bipartition of a 6-site random MPS and its disentangled forms, computed via the SSO algorithm and the loss function defined in Eq. 14. In this example, the target MPS has $F_{\chi=2} = 0.8356$ and the disentangled state after $L = 10$ layers has $F_{\chi=2} = 0.9998$.

where $|\psi^{(L)}\rangle$ is designed to be well approximated by a $\chi = 2$ MPS $|\tilde{\psi}^{(L)}\rangle$. The corresponding fidelity of this low-rank approximation is

$$F_L := |\langle \psi^{(L)} | \tilde{\psi}^{(L)} \rangle|^2 \quad (16)$$

To reverse the disentangling process, we first prepare $|\tilde{\psi}^{(L)}\rangle$ using

$$U_{\text{prep}} |0\rangle^{\otimes n} = |\tilde{\psi}^{(L)}\rangle \quad (17)$$

where U_{prep} can be computed exactly by embedding the tensors of $|\tilde{\psi}^{(L)}\rangle$ into a single layer of $SU(4)$ gates (i.e., the exact same circuit form of a single layer of the staircase ansatz in Eq. 12). Then, the full state preparation circuit is given by

$$U_S := U_1^\dagger U_2^\dagger \cdots U_L^\dagger U_{\text{prep}} \quad (18)$$

such that $U_S |0\rangle^{\otimes n}$ prepares an approximation of the original target $|\psi^{(1)}\rangle$. See Fig. 4 for a visualisation, noting that the sequential circuit structure allows for operations to be run in parallel across all qubits. Conveniently, this is exactly the same structure as the circuit computed by the MPD algorithm [18], allowing for a direct comparison of the methods. By unitarity, the fidelity of the approximate state prepared by U_S is exactly

$$|\langle \psi^{(1)} | U_S | 0^{\otimes n} \rangle|^2 = |\langle \psi^{(L)} | \tilde{\psi}^{(L)} \rangle|^2 = F_L \quad (19)$$

Thus, minimising the loss in Eq. 14 directly maximises the fidelity of the final prepared state with the target, subject to the shallow-depth constraint. Note that the addition of the U_{prep} layer implies that a

target circuit depth of L layers should include only $L - 1$ *optimised* layers.

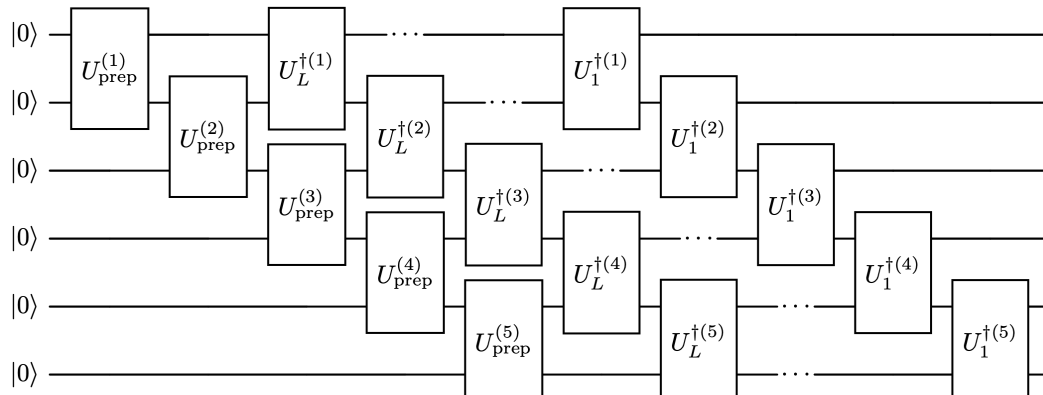


FIG. 4: The quantum circuit generated by the SSO algorithm for L optimised layers and 6 qubits, showing how each staircase-like layer can be parallelised. The output of the circuit is an approximation of the target MPS.

4.4 Fidelity-Maximising Post-Processing

In the SSO algorithm, each layer is optimised in isolation while keeping the parameters of all other layers fixed. The SSO is therefore greedy in the sense that each layer minimises the loss in Eq. 14 without “planning ahead”. This significantly increases the likelihood of local minima. As such, it is possible to improve the fidelity of the prepared state by *jointly* optimising all layers as a post-processing step. The fidelity-maximising loss function is defined as

$$F(\theta_{1:L}) = |\langle \psi^{(1)} | U_S(\theta_{1:L}) | 0^{\otimes n} \rangle|^2 \quad (20)$$

where $U_S(\theta_{1:L})$ represents the circuit consisting of all L parameterized layers (including U_{prep}). The parameters $\theta_{1:L}$ are initialised to be exactly those computed by the SSO algorithm. We denote this algorithm as SSO+All.

Unless efficient bond dimension truncations can be made in the contraction of the L circuit layers, the bond dimension required to compute the loss in Eq. 20 scales as $\chi_{\max} = \mathcal{O}(2^L)$. Moreover, collective optimisation of deep tensor network circuits is known to suffer from severe local minima problems and loss landscapes mirroring barren plateaus as depth is increased [19, 20]. These effects are, however, diminished when the training is *initialised* by high-quality parameters [2, 28]. This implies that SSO+All can be efficiently trained for small numbers of layers L , and is particularly well-suited to near-term quantum implementation. In Section 5, we show that initialising the parameters $\theta_{1:L}$ using the SSO algorithm significantly improves training outcomes compared to initialisation using the MPD algorithm.

4.5 Complexity Analysis

Time complexity. For an n -qubit target MPS $|\psi^{(1)}\rangle$ disentangled by L layers with T optimisation iterations per layer, the overall complexity of the SSO algorithm is

$$\mathcal{O}(T n^2 L \chi_{\max}^3)$$

where χ_{\max} denotes the maximum bond dimension reached by any intermediate state during the disentangling process. The cubic dependence on χ_{\max} arises from the $\mathcal{O}(n\chi_{\max}^3)$ cost of computing Schmidt

decompositions (or, equivalently, performing local SVDs) across the $n - 1$ bonds of the MPS at each optimisation step.

Each circuit layer $U_k(\theta_k)$ can be viewed as the $\chi = 2$ instance of an MPU [26]. When such a layer is contracted with an intermediate MPS $|\psi^{(k)}\rangle$ of bond dimension $\chi^{(k)}$, the resulting state $|\psi^{(k+1)}\rangle$ has bond dimension $\chi^{(k+1)} = 2\chi^{(k)}$ before any truncation. Naïvely, this implies that the maximum bond dimension scales as $\chi_{\max} = \mathcal{O}(2^L \chi_{\text{targ}})$, so that the worst-case time complexity of the disentangling procedure would scale as $\mathcal{O}(8^L)$ in L . In SSO, however, each layer $U_k(\theta_k)$ is explicitly optimised to *disentangle* $|\psi^{(k)}\rangle$, so that in practice $|\psi^{(k+1)}\rangle$ can be truncated back to a much smaller bond dimension with negligible error. Hence, the scaling of χ_{targ} must be investigated empirically.

Maximum bond dimension scaling. As we show in Section 5, the extent to which the bond dimension can be truncated after each layer is directly tied to how effectively $U_k(\theta_k)$ reduces entanglement. To investigate this, we employ a simple truncation rule in which all Schmidt values satisfying $\lambda_{i,j}^{(k+1)} \leq \lambda_{\text{thresh}}$ are discarded. In our experiments we set $\lambda_{\text{thresh}} = 10^{-7}$, ensuring that the truncation error is extremely small. For all SSO test cases considered, we observe that $\chi_{\max} = \mathcal{O}(\chi_{\text{targ}})$, i.e., the exponential growth in bond dimension with L is completely avoided. This stands in sharp contrast to the MPD algorithm, where ineffective disentangling can lead to inefficient scaling of χ_{\max} , a claim which we substantiate in Section 5.

More aggressive truncation strategies can, in principle, further reduce the cost of SSO. For example, choosing a larger threshold λ_{thresh} reduces χ_{\max} at the expense of increasing the truncation error (cf. Eq. 10) and thereby introducing an irreducible approximation error into the disentangling process. The optimal choice of λ_{thresh} is problem-dependent, and in practice one may prefer adaptive schemes that adjust the allowed bond dimension dynamically based on local truncation errors or target accuracies. From a numerical perspective, the explicit control over Schmidt spectra and truncation thresholds also contributes to stable optimisation, preventing the ill-conditioned growth in bond dimension that can plague fidelity-maximising TNO approaches.

It is useful to contrast this behaviour with TNO schemes that treat the full L -layered circuit $U(\theta_{1:L}) = U_L(\theta_L) \cdots U_1(\theta_1)$ as a single variational object and optimise all layers jointly to maximise the fidelity $F(\theta_{1:L}) = |\langle \psi_{\text{targ}} | U(\theta_{1:L}) | 0^{\otimes n} \rangle|^2$. The composed circuit $U(\theta_{1:L})$ is itself an isometric tensor network whose bond dimension grows as $\chi_{\text{circ}} = 2^L$ in the worst-case. Evaluating $F(\theta_{1:L})$ and its gradients exactly then requires contracting an MPS of bond dimension χ_{circ} with the target MPS, leading to a per-iteration cost that scales as $\mathcal{O}(n \chi_{\text{circ}}^3) = \mathcal{O}(n 8^L)$. In practice, one must introduce truncations after intermediate layers to keep χ_{circ} manageable, but this couples approximation error directly to the optimisation dynamics. Hence, joint optimisation of all layers as a post-processing step is best-suited to shallow-depth circuits.

5. Results and Discussion

Algorithms. In this section, we empirically assess the performance of Schmidt Spectrum Optimisation (SSO) against the Matrix Product Disentangler (MPD) [18] and its optimised variants [2, 3]. These variants differ by optimisation approach. First, we denote a layerwise optimisation approach using a fidelity-maximising loss function as MPD+LW. In MPD+LW, we first compute the MPD algorithm before optimising each circuit layer in isolation while keeping all other layers fixed. This is analogous to the layerwise optimisation strategy employed in SSO. We also implement MPD+All, which is where the circuit layers computed by MPD+LW are then *jointly* optimised together to maximise fidelity. This is the same

Method	Loss Function	Opt-Layerwise	Opt-All	Parameter Init.	Complexity*
MPD [18]	–	–	–	None	$\mathcal{O}(nL\chi_{\max}^3)$
SSO	Schmidt Spectra	✓	–	Identity	$\mathcal{O}(Tn^2L\chi_{\max}^3)$
MPD+LW [2]	Fidelity	✓	–	MPD	$\mathcal{O}(TnL\chi_{\max}^3)$
MPD+All [2, 3]	Fidelity	✓	✓	MPD+LL	$\mathcal{O}(T^2nL\chi_{\max}^3)$
SSO+All	Schmidt + Fidelity	✓	✓	SSO	$\mathcal{O}(T^2n^2L\chi_{\max}^3)$

TABLE I: Definitions of Compared Methods.

* T denotes training iterations, n qubits, L layers, and χ_{\max} maximum MPS bond dimension. Note that χ_{\max} is a crucial parameter in the complexity, and the scaling of χ_{\max} differs significantly depending on the state preparation methodology. For example, we show that SSO leads to a significantly reduced χ_{\max} relative to MPD-based methods.

fidelity-maximising post-processing step described in Section 4.4. Lastly, we implement SSO+All, which is implements fidelity-maximisation as a post-processing step using the output from the SSO algorithm to initialise parameters. See a summary of these methods in Table I.

Overview. We benchmark the SSO on MPS approximations to ground states of four lattice Hamiltonians. We present the accuracy of the state preparation procedures in terms of the fidelity of the prepared state, defined as $F_S = |\langle \psi_{\text{targ}} | U_S | 0^{\otimes n} \rangle|^2$ for each state preparation circuit U_S computed across different numbers of layers. The state preparation error (infidelity) is then $\epsilon_S = 1 - F_S$. Alongside these plots we report the scaling of the bond dimension χ_{\max} for the SSO and MPD algorithms using a Schmidt coefficient threshold of $\lambda_{\text{thresh}} = 10^{-7}$ to truncate the bond dimension of each layer after disentangling.

For this shallow-depth case study, we do *not* constrain the bond dimension χ_{\max} of the optimised variants, meaning that $\chi_{\max} \sim 2^L$ for these TNO variants. See Section 4.5 for a more nuanced discussion around how to deal with χ_{\max} in these cases, especially for deeper circuits. In essence, setting a maximum χ_{\max} in TNO results in a coupling of a compression approximation with the optimal dynamics. We choose not to constraint χ_{\max} for these optimised variants to prevent this coupling effect from confounding results.

Empirical assessment. We first benchmark on the 48-qubit quantum site Ising chain in a transverse field,

$$H = - \sum_{i=1}^{n-1} Z_i Z_{i+1} - h_x \sum_{i=1}^n X_i \quad (21)$$

with $n = 48$, $J = 1.0$, $h_x = 0.5$, and open boundary conditions (i.e. the system is inside the gapped ferromagnetic phase). The target bond dimension is $\chi_{\text{Ising}} = 10$. For the quantum Ising model, we only compare the SSO algorithm against the MPD algorithm, illuminating a monumental difference in performance. In this case, the MPD algorithm exhibits highly pathological behaviour, with χ_{\max} growing nearly exponentially while the disentangling procedure is largely ineffective. On the other hand, the MPS permits a $\chi = 4$ approximation with $F_{\chi=4} = 0.9836$ fidelity, and the SSO optimises to $F = 0.9980$ within just 2 layers (i.e., only a *single* optimised layer followed by its $\chi = 2$ approximation that we denote by $|\tilde{\psi}^{(L)}\rangle$). This greedy optimisation does, however, appear to approach a local minima solution, evidenced by the plateauing gains in fidelity with increasing circuit layers.

Next, we benchmark on target MPS approximations to the ground-states of three other lattice Hamiltonians. As a disordered spin model in the many-body localised regime, we consider an $n = 16$ -site

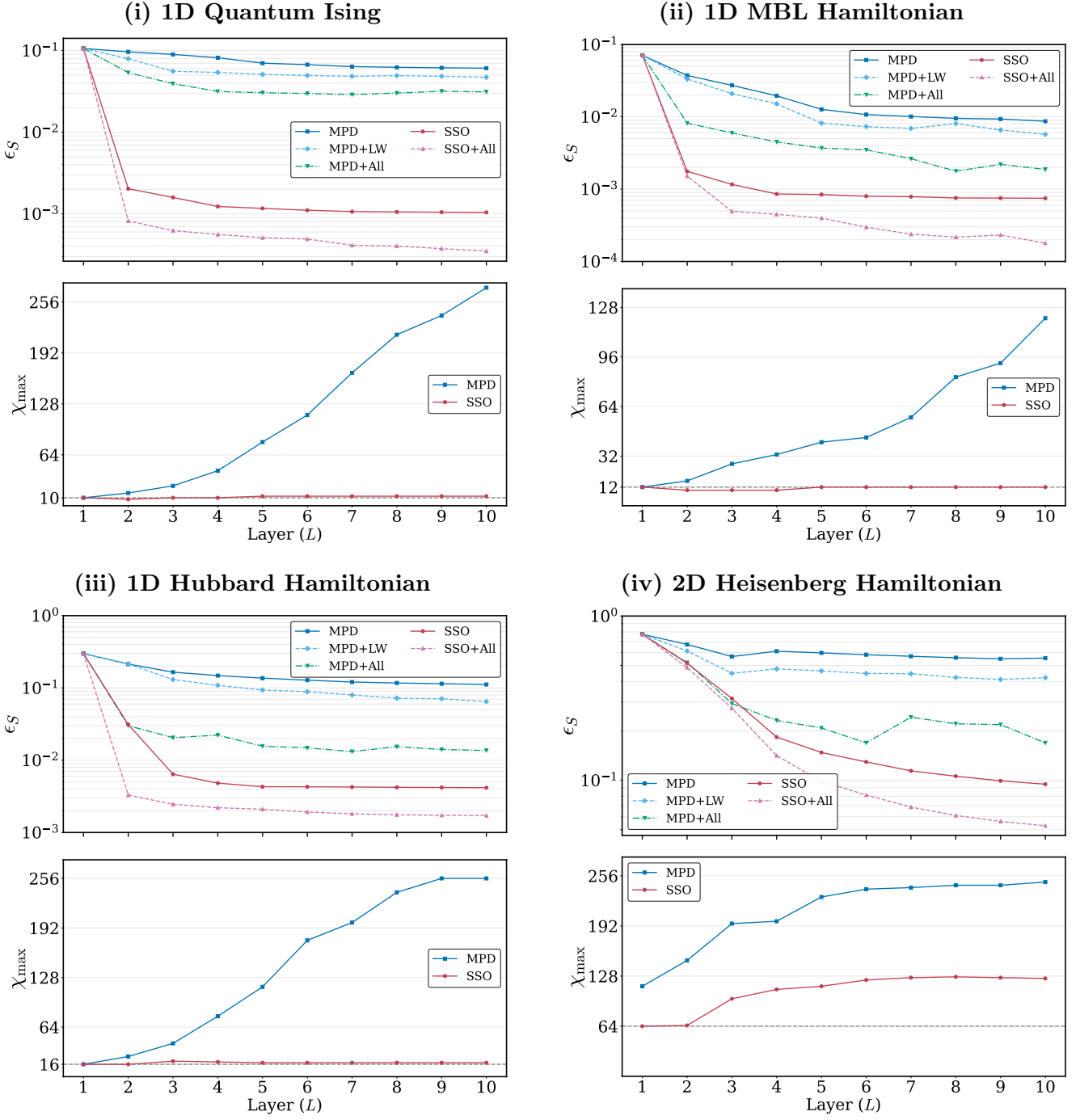


FIG. 5: The performance of the SSO algorithm and its post-processed version (SSO+All) with the MPD and its optimised variants. We test across four MPS approximations of the ground-states of lattice Hamiltonians: (i) The 1D quantum Ising model near-criticality with $n = 48$ qubits, (ii) A disordered spin model in the many-body localised regime with $n = 16$ qubits, (iii) The spinless Hubbard Chain with $n = 16$ qubits, and (iv) The 2D Heisenberg with nearest-neighbour coupling on a 4×4 grid of qubits. *Above plot:* the state preparation error $\epsilon_S = 1 - F_S$ across layers L , where F_S is the fidelity between the simulated circuit output and the target MPS. *Below plot:* the scaling of χ_{\max} during disentangling using $\lambda_{\text{thresh}} = 10^{-7}$. Best of 2 runs reported.

spin- $\frac{1}{2}$ chain with random longitudinal fields of strength $dh = 1.0$ drawn from a Gaussian distribution ($\chi_{\text{MBL}} = 10$). As a one-dimensional fermionic model, we use the spinless Hubbard chain with $n = 16$ sites, hopping amplitude $t = 0.5$, nearest-neighbour interaction strength $V = 1.0$, and chemical potential

$\mu = 1.0$, with open boundary conditions ($\chi_{\text{Hubbard}} = 16$). Finally, we study the spin- $\frac{1}{2}$ 2D Heisenberg model on a 4×4 square lattice with nearest-neighbour coupling $J = 1.0$ and open boundary conditions ($\chi_{\text{Heisenberg}} = 64$).

In all test cases, the SSO reduced the error in the prepared state by approximately an order of magnitude compared to the MPD. Simultaneously, the SSO algorithm mitigates the unfavourable scaling of χ_{max} emerging from the ineffective disentangling of the MPD algorithm. In addition, SSO alone outperforms all optimised variants of MPD, including the jointly optimised and pre-trained MPD+All algorithm. This provides lucid evidence that these TNO variants suffer from subpar local minima, and that it's possible to improve training outcomes using improved optimisation strategies.

Lastly, the SSO+All algorithm performs the best across all test cases. This is unsurprising: since the parameters are initialised by the output of SSO, the *worst-case* performance of SSO+All is exactly equal to that of SSO. In reality, we find that the joint optimisation of layers often significantly improves outcomes. At deeper layers, however, the joint optimisation plateaus (and sometimes worsens e.g. see MPD+All in Fig. 5(iv)). Despite the circuit being *deeper*, the optimisation process is unable to exploit the additional expressivity of the circuit, largely because the parameter initialisation has only marginally improved while deeper circuits significantly increase the likelihood of finding suboptimal local minima [20]. In any case, it is clear from the comparative performance of the MPD+All and SSO+All algorithms that the quality of the parameter initialisation plays a critical role in mitigating the effects of local minima when traversing the loss landscape.

6. Discussion and Conclusions

In this work, we introduced a new protocol, Schmidt Spectrum Optimisation (SSO), for the disentangling and preparation of Matrix Product States (MPS). The SSO algorithm iteratively optimises layers of one- and two-qubit gates, represented as tensor networks (MPUs), to sequentially disentangle a given MPS. The optimisation process extremises a loss function defined explicitly on the Schmidt spectra of the iteratively updated, disentangled MPS. The specific choice of loss function adopted in our work corresponds to minimising the $\chi = 2$ truncation error of each intermediate state in the disentangling process. We showed how reversing this process generates a quantum state preparation circuit, the fidelity of which exactly corresponds to the $\chi = 2$ fidelity of the final, least entangled state in the process. The full algorithm has time complexity $\mathcal{O}(Tn^2L\chi_{\text{max}})$ for L layers, and the optimisation is computed entirely classically.

We demonstrated that SSO significantly improves upon its non-optimised predecessor, the Matrix Product Disentangler (MPD) [18]. By uniquely re-framing the disentangling process as an iterative optimisation problem, we compute effective disentangling layers that keep χ_{max} small while quickly removing entanglement from the state, subject to the expressivity of the circuit operators. The advantage is two-fold: (i) each disentangling layer is more effective, leading to higher-quality quantum state preparation circuits, and (ii) the empirical scaling of χ_{max} was shown to be far superior to existing methods, enabling the efficient computation of deeper circuits. In addition, the SSO algorithm significantly outperformed the optimised variant in all test cases. We also showed that applying a joint optimisation of the circuit operators computed by the SSO algorithm (i.e., SSO+All), leads to further improvements.

In fidelity-maximising TNO approaches (MPD+LW and MPD+All), each optimisation step is constrained to keep the output state of the circuit close to the target MPS. The SSO algorithm relaxes this

constraint, and the circuit output state is allowed to explore a larger state space while searching for states that further minimises the Schmidt spectrum loss function. Additionally, SSO is computed *backwards* by disentangling from the target state, rather than the typical *forward* optimisation approach, where each layer (starting from the computational all-zero state) is optimised to progressively rebuild the entanglement of the target MPS. The backwards approach alleviates some of the path-dependent pathologies typical of the forwards approach, where greedily maximising fidelity at a given layer fails to “plan ahead” and fidelity gains quickly plateau.

The fidelity-maximising optimisation initialised by the SSO algorithm, i.e. SSO+All, generated the highest fidelity state preparation circuits across all experiments. It’s notable that the only algorithmic difference between MPD+All and SSO+All is the contrasting use of the MPD and SSO algorithms to initialise the circuit parameters. In all cases, the better parameter initialisation by SSO led to *significantly* improved local minima found when all layers are jointly optimised. We therefore also contribute to the growing body of literature exploring the crucial role of “warm-start” parameter initialisations when training quantum parametrised circuits and tensor network optimisations alike [28].

The core limitation of the SSO approach lies in the prevalence of suboptimal local minima during optimisation. We found that local minima can cause the state preparation fidelity to plateau at larger numbers of layers, despite the increased expressivity of the quantum circuit. In experimentaiton, we found that the risk of local minima increased with χ_{targ} , reflecting the increased complexity of navigating high-dimensional TN parameter landscapes. This limitation was also characteristic of all other TNO methods explored [2, 3, 7, 19]. While we partially mitigated this effect using basin-hopping, future work could explore more sophisticated approaches to avoiding local minima during TNO.

To the best of our knowledge, this is the first work that has successfully engineered a loss function defined explicitly on the Schmidt spectra of a tensor network state. The stable computation of gradients, however, relied on the capability to auto-differentiate through the MPS and MPU contraction, as well as the subsequent computation of Schmidt decompositions. It is a core question as to whether this approach can scale to other isometric tree-like tensor network structures, such as the binary Tree Tensor Network (bTTN), which have greater expressive power compared to the MPS ansatz [8]. Future work may also consider how the Schmidt loss function can be modified to improve performance. For example, can we more explicitly regularise against the growth of χ_{max} during training? What adjustments can be made to the training process or loss function to reduce the effects of local minima? Moreover, how does our approach compare to, say, maximising the $\chi = 4$ truncation error at the next layer followed by a small decomposition of a 3-qubit gate layer?

In conclusion, the SSO provides a novel approach to quickly and iteratively disentangling an MPS using layers of local $SU(4)$ gates by extremising a loss function defined explicitly on the Schmidt spectra of the disentangled state. The disentangling process can be easily reversed by computing the adjoints of the disentangling layers, meaning that SSO can be used to generate highly efficient quantum state preparation circuits. We demonstrated substantial improvements over existing methods across a range of ground-state MPS approximation benchmarks, reducing the encoding error by up to an order of magnitude while simultaneously improving the scaling of time-complexity with increasing circuit depth.

[1] C. Schön, E. Solano, F. Verstraete, J. I. Cirac, and M. M. Wolf, Sequential generation of entangled multiqubit states, *Phys. Rev. Lett.* **95**, 110503 (2005).

[2] M. S. Rudolph, J. Chen, J. Miller, A. Acharya, and A. Perdomo-Ortiz, Decomposition of matrix product states into shallow quantum circuits, *CoRR* **abs/2209.00595**, 10.48550/arXiv.2209.00595 (2022).

[3] M. Ben-Dov, D. Shnaiderov, A. Makmal, and E. G. Dalla Torre, Approximate encoding of quantum states using shallow circuits, *npj Quantum Information* **10**, 65 (2024).

[4] J. Iaconis, S. Johri, and E. Y. Zhu, Quantum state preparation of normal distributions using matrix product states, *npj Quantum Information* **10**, 15 (2024).

[5] D. Malz, G. Styliaris, Z. Wei, and J. Cirac, Preparation of matrix product states with log-depth quantum circuits, *Physical Review Letters* **132**, 040404 (2024).

[6] K. C. Smith, A. Khan, B. K. Clark, S. Girvin, and T. Wei, Constant-depth preparation of matrix product states with adaptive quantum circuits, *PRX Quantum* **5**, 030344 (2024).

[7] A. Melnikov, A. Termanova, S. Dolgov, F. Neukart, and M. Perelshtain, Quantum state preparation using tensor networks, *Quantum Science and Technology* **8**, 035027 (2023).

[8] S. Sugawara, K. Inomata, T. Okubo, and S. Todo, Embedding of tree tensor networks into shallow quantum circuits, *CoRR* **abs/2501.18856**, 10.48550/arXiv.2501.18856 (2025).

[9] G. Vidal, Class of quantum many-body states that can be efficiently simulated, *Phys. Rev. Lett.* **101**, 110501 (2008).

[10] Z.-Y. Wei, D. Malz, and J. I. Cirac, Sequential generation of projected entangled-pair states, *Phys. Rev. Lett.* **128**, 010607 (2022).

[11] F. Verstraete and J. I. Cirac, Matrix product states represent ground states faithfully, *Phys. Rev. B* **73**, 094423 (2006).

[12] J. Eisert, M. Cramer, and M. B. Plenio, Colloquium: Area laws for the entanglement entropy, *Reviews of Modern Physics* **82**, 277 (2010).

[13] E. Stoudenmire and S. R. White, Studying two-dimensional systems with the density matrix renormalization group, *Annual Review of Condensed Matter Physics* **3**, 111 (2012).

[14] G. Ehlers, S. R. White, and R. M. Noack, Hybrid-space density matrix renormalization group study of the doped two-dimensional hubbard model, *Phys. Rev. B* **95**, 125125 (2017).

[15] S. R. White and D. J. Scalapino, Density matrix renormalization group study of the striped phase in the 2d hubbard model, *Phys. Rev. Lett.* **80**, 1272 (1998).

[16] M. Möttönen, J. J. Vartiainen, V. Bergholm, and M. M. Salomaa, Quantum circuits for general multiqubit gates, *Phys. Rev. Lett.* **93**, 130502 (2004).

[17] A. M. Krol, A. Sarkar, I. Ashraf, Z. Al-Ars, and K. Bertels, Efficient decomposition of unitary matrices in quantum circuit compilers, *Applied Sciences* **12**, 10.3390/app12020759 (2022).

[18] S.-J. Ran, Encoding of matrix product states into quantum circuits of one- and two-qubit gates, *Phys. Rev. A* **101**, 032310 (2020).

[19] J. Green and J. B. Wang, *Quantum encoding of structured data with matrix product states* (2025), arXiv:2502.16464 [quant-ph].

[20] Z. Liu, L.-W. Yu, L.-M. Duan, and D.-L. Deng, Presence and absence of barren plateaus in tensor-network based machine learning, *Phys. Rev. Lett.* **129**, 270501 (2022).

[21] R. Orús, A practical introduction to tensor networks: Matrix product states and projected entangled pair states, *Annals of Physics* **349**, 117 (2014).

[22] I. V. Oseledets, Tensor-train decomposition, *SIAM Journal on Scientific Computing* **33**, 2295 (2011).

[23] U. Schollwöck, The density-matrix renormalization group in the age of matrix product states, *Annals of Physics* **326**, 96 (2011).

[24] L. Mirsky, Symmetric gauge functions and unitarily invariant norms, *Quarterly Journal of Mathematics* **11**,

50 (1960).

- [25] C. Eckart and G. Young, The approximation of one matrix by another of lower rank, *Psychometrika* **1**, 211 (1936).
- [26] G. Styliaris, R. Trivedi, D. Perez-Garcia, and J. I. Cirac, Matrix-product unitaries: Beyond quantum cellular automata, *Quantum* **9**, 1645 (2025).
- [27] A. Paszke, S. Gross, S. Chintala, G. Chanan, E. Yang, Z. DeVito, Z. Lin, A. Desmaison, L. Antiga, and A. Lerer, Automatic differentiation in pytorch, in *NIPS 2017 Workshop on Autodiff* (2017).
- [28] E. Grant, L. Wossnig, M. Ostaszewski, and M. Benedetti, An initialization strategy for addressing barren plateaus in parametrized quantum circuits, *Quantum* **3**, 214 (2019).